Benjamin DAGUSÉ[1,2], Philippe DESSANTE[1], Pierre VIDAL[1], Jean-Claude VANNIER[1], Jacques SAINT-MICHEL[2], Jean-Luc THOMAS[1]

Supélec (1), Moteurs Leroy Somer (2)

Optimization and Comparison of Optimal Saliency Permanent Magnet Synchronous Machines for Electric Vehicle Application

***Abstract**. For electric vehicles' traction, Permanent Magnet Synchronous Machines (PMSM) are interesting because of their high power density and their efficiency on a large flux weakening range. This solution offers multi-possibilities of conception. As a matter of fact, it is possible to choose surface or saliency PMSMs, this last one could be dissociate into two groups: Normal-Saliency PMSM and Inverse-Saliency PMSM. Based on a typical working cycle of electric vehicles, we will compare optimal Normal-Saliency PMSM and Inverse-Saliency PMSM performances.*

Streszczenie.** Silniki synchroniczne z magnesem trwałym dobrze działają w pojazdach trakcyjnych, co wynika z ich dużej gęstości mocy a także z ich efektywności w osłabianiu strumienia w dużym zakresie. Tego rodzaju rozwiązanie oferuje wiele możliwości. W zasadzie istnieje możliwość wyboru pomiędzy powierzchniowymi a występowymi maszynami, przy czym te ostatnie mogą być podzielone na dwie grupy: maszyny o występie normalnym i przeciwnym. W pracy przedstawiono porównanie obu tych optymalnych rozwiązań, bazując na typowym cyklu pracy pojazdów elektrycznych. **(Optymalizacja i porównanie maszyn synchronicznych z magnesem trwałym o optymalnym występie dla pojazdów elektrycznych).

Keywords: Permanent magnet synchronous machine, Optimization, Electric vehicle application.
Słowa kluczowe: maszyna synchroniczna z magnesem trwałym, optymalizacja, zastosowanie w pojazdach elektrycznych

Introduction

Within the context of electric vehicle and hybrid electric vehicle development [1], the value of the current supplying the machine is an important criterion as it is directly related to the vehicle autonomy. Permanent Magnet Synchronous Machines (PMSM) are particularly attractive because of their high power density and their efficiency on a large flux weakening range [2-3].

The electric vehicle or hybrid electric vehicle working cycles [4] are described by the vehicle speed vs. time characteristic and the motor torque vs. time characteristic. These characteristics give the motor power, torque and speed through a conversion done by the gearbox.

Based on some motor working points and the PMSM model, an optimization of the electromagnetic parameters is carried out. The optimization objective is to minimize the current consumption for both saliencies. This leads to a comparison between Normal-Saliency PMSM and Inverse-Saliency PMSM for a typical electric vehicle cycle and allows quantifying the savings. Another goal is to emphasize the electromagnetic parameters combination for minimizing the objective function and show their values.

Electric vehicle working cycle and strategies

The on road electric vehicle characteristics are described in Fig. 1 which gives vehicle's speed in kilometer per hour as well as the electric motor's torque. This corresponds to a typical working urban and freeway configurations of the vehicle.

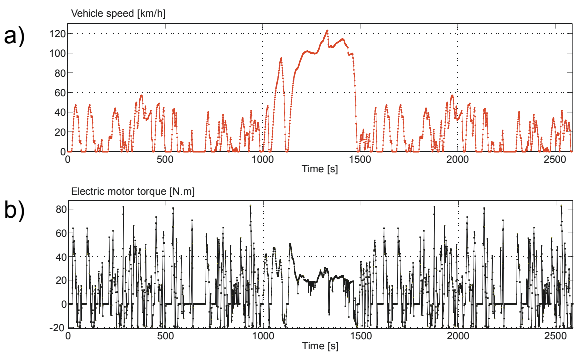

Fig.1. *a)* Vehicle speed, *b)* Electrical motor torque

From this working cycle, each point of Fig. 1. is set in the motor's characteristics (power vs. speed and torque vs. speed).

For the motor, the constraints are defined by the maximum power *Pmax*, the maximum torque *Tmax*, the base speed ω_b and the flux-weakening capability. In our case, classical boundaries are employed to set the maximum characteristics [5]:

- At start, a constant maximum torque until maximum power is reached;
- P_{max} and T_{max} define the base point where speed is equal to ω_b;
- To finish, a constant-power speed range on the flux weakening range.

The motor's operating points are reported in power vs. speed characteristic and torque vs. speed characteristic (Fig. 2). Boundaries (red lines) must be respected, they will be introduced in the optimization constraints.

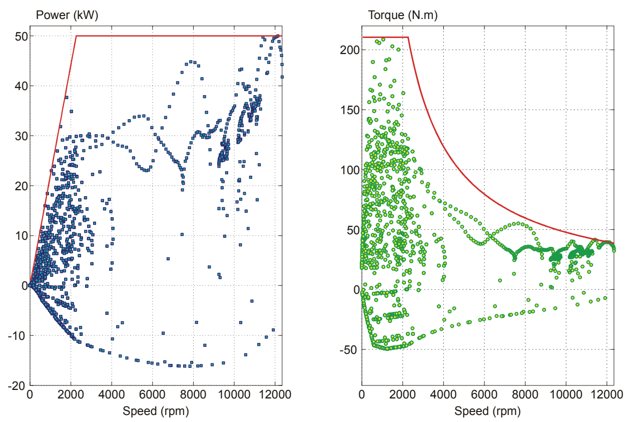

Fig.2. Functioning points and boundaries in power-speed and torque-speed ranges

In a context of optimization, an evaluation of each operating point is very time consuming, thus a reduction of the number of points is necessary. A clustering procedure determines the centroids of each cluster. A centroid is defined by its coordinates in the power vs. speed characteristic and its weight is equal to the number of cluster's operating points. Results of this procedure are illustrated in Fig. 3 where each cluster is showed by a specific color and its centroid (black cross).

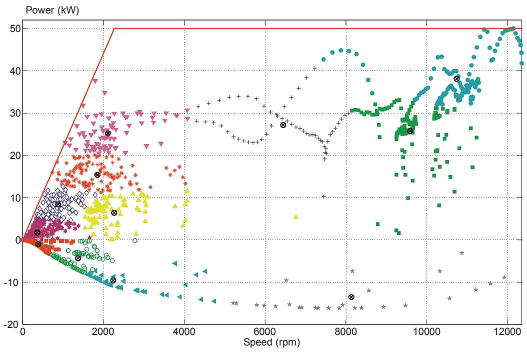

Fig.3. Clusters and centroids in the power vs. speed characteristic

With this procedure, the objective function for this optimization problem is reduced at 12 evaluations versus about 2 000 evaluations initially.

Assumptions and PMSM Model

In performances' criterions, the PMSM is particularity adapted for vehicle's traction thanks to its efficiency on a large flux weakening range compared with other machines [6-7].

The PMSM analytical model included some simplifying assumptions: the winding resistance is neglected, the saturation effects are not taken into account and the stator reaction is ignored. The second assumption allows considering the electromagnetic parameters proportional to the speed or to the frequency. Thus, the electromagnetic parameters – *E* the ElectroMotive Force (EMF), X_d and X_q respectively the reactances in *d*-axis and *q*-axis – are proportional to the speed. The introduction of the speed ratio *m* allows explaining these three parameters - defined to the base point - as constants on the speed range.

(1) $$m = \frac{\omega}{\omega_b} = \frac{f}{f_b}$$

(2) $$\begin{cases} E = m.E_b \\ X_d = m.X_{db} \\ X_q = m.X_{qb} \end{cases}$$

As in [8], electromagnetic quantities like *EMF* and reactances in *dq*-axis are used in the analytical modelling of the PMSM by relationships of power, voltage, and current. Following the previous assumptions and with (1) and (2), the equations for each phase in steady-state operation are:

(3) $$P = m.\left(E_b.I_q + \left(X_{db} - X_{qb}\right)I_d.I_q\right)$$

(4) $$V = m.\sqrt{\left(E_b - X_{db}.I_d\right)^2 + \left(X_{qb}I_q\right)^2} \quad \leq \quad \left(V_{max}\right)$$

(5) $$I = \sqrt{I_d{}^2 + I_q{}^2}$$

where V_{max}, the maximum voltage per phase, is a function of the PWM maximum *dc*-voltage.

In the following, we will not write the "*b*" sign for *E*, X_d and X_q which are the electromagnetic parameters at the base point.

PMSM could be classified into three groups defined by the saliency ratio between reactances *d* and *q*. In [9], the saliencies are defined as follows:

- Non-Saliency with $X_d/X_q \approx 1$ *(for example Surface PMSM)*;
- Normal-Saliency by $X_d/X_q > 1$;
- Inverse-Saliency by $X_d/X_q < 1$.

The electromagnetic parameters have an important impact because they impose the rotor design and the magnets' configuration [10].

Optimization Procedure

The optimization aim is to minimize the current values by the batteries during the operating cycle. The PMSM's relationships are coupled with an algorithm where the electromagnetic parameters are the variables of the optimization. A Genetic Algorithm (GA) is employed to solve this optimization problem. With one set of parameters, the minimal current is calculated for each centroid defined by its power, speed and weight. Then, the objective function is evaluated and returned at the GA.

Electromagnetic Parameters' Boundaries

The boundaries of electromagnetic parameters (Table 1.) are logically the same for both optimization problems, except the saliency ratio.

Table 1. Boundaries of the optimization

Parameter	Value	Unit
E (ElectroMotive Force)	[0 ; 133.3]	V
X_d (reactance *d*-axis)	[0.01 ; 10]	Ω
X_q (reactance *q*-axis)	[0.01 ; 10]	Ω
Normal-Saliency (Xd>Xq)		
X_d/X_q	[1 ; 3]	-
Inverse-Saliency (Xd<Xq)		
X_d/X_q	[1/3 ; 1]	-

In order to compare Saliency PMSM and to estimate the gap between them, we choose to run two separates optimizations. Thus two optimal machines will be compared: Normal-Saliency vs. Inverse-Saliency PMSM.

Optimization Results

The characteristics of the optimal machines are given in Table 2. It needs 90 individuals and 97 iterations (Fig.4.).

Table 2. Optimization' results comparison

Normal-Saliency (Xd>Xq)	
E	133.3 V
X_d	1.788 Ω
X_q	0.596 Ω
X_d/X_q	3
Objective function	5.26e2
Inverse-Saliency (Xd<Xq)	
E	133.3 V
X_d	1.625 Ω
X_q	4.876 Ω
X_d/X_q	1/3
Objective function	4.76e2

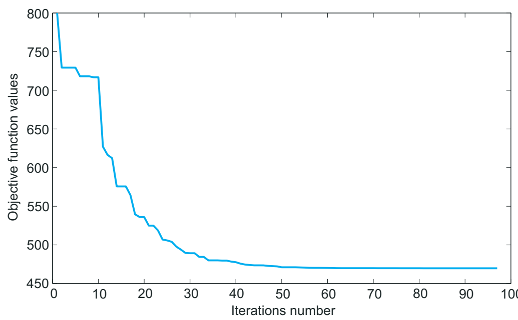

Fig.4. Evolution of the objective function for the Inverse Saliency optimization

With these optimal electromagnetic parameters (E, X_d and X_q) for Normal-Saliency and Inverse-Saliency PMSM, we can estimate the current consumption on the complete power-speed characteristic. We choose to calculate current only on motor working (Fig.5. and Fig.6.) and to compare the gap in percentage of two optimal saliencies machines.

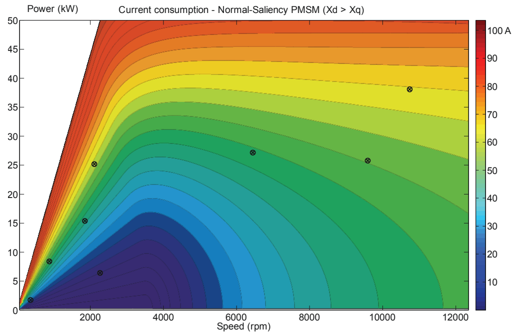

Fig.5. Current consumption for Normal-Saliency PMSM

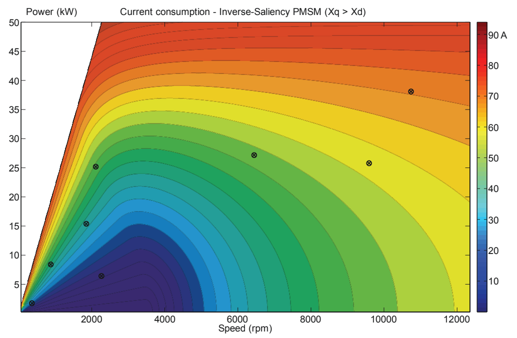

Fig.6. Current consumption for Inverse-Saliency PMSM

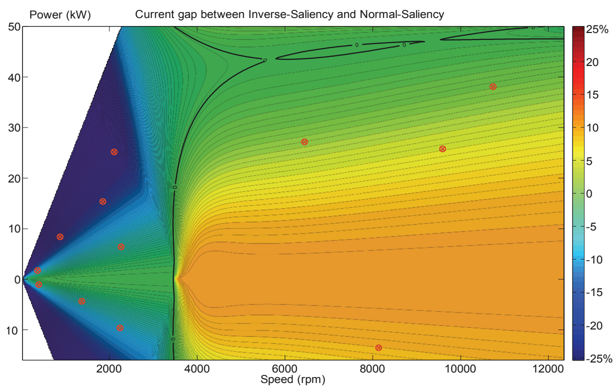

Fig.7. Gap of current consumption between Inverse-Saliency and Normal-Saliency (black lines indicate the zero consumption gap)

Results of the optimization (Table 2.) are given for both cases, the *EMF* is maximized and the saliency ratio is maximized for Normal-Saliency and minimized for the Inverse-Saliency. Finally, whatever the saliency, optimizations strive to maximize the *EMF* value and the difference between the reactances. Moreover, with this procedure, we obtained the values of the reactances, solutions of optimal machines.

The results of the minimization of objective functions show that the Inverse-Saliency is better than the Normal-Saliency (about 11%). Thus, the first have a current consumption lower that the second, so compared to the Normal-Saliency, the Inverse-Saliency is better at maximizing the vehicle's autonomy.

Moreover, maximal current obtained in Fig.5. and Fig.6. is lower for Inverse-Saliency with 94A vs. 104A for Normal-Saliency PMSM. This gap of about 10% is an important criterion for the maximal admissible current of the inverter. Therefore, size of electronic components can be reduced.

The complete power-speed characteristic (Fig.7.) gives the gap ε of current consumption for optimal machines (6), where blue gradation indicate that the current consumed by Inverse-Saliency is lower than that of Normal-Saliency. On the opposite, the current consumed by Inverse-Saliency is lower on the red gradation.

$$\varepsilon_{[\%]} = \frac{I_{Inverse-Saliency} - I_{Normal-Saliency}}{I_{Normal-Saliency}} \times 100 \qquad (6)$$

We can see that the Inverse-Saliency is more efficient on the constant torque range with a gap of about 25% (blue). Conversely, on the flux weakening range, the Normal-Saliency give better results; however, maximum gap is only of 10% (orange).

Finally all results prove that the Inverse-Saliency PMSM is the better for VE application with a lower maximal current and a better current consumption on the complete cycle.

Conclusion

The study on the operating cycle permitted to reduce significantly the number of evaluations. Thus, we used clusters to group cycle operating points at a centroid defined by its coordinates and its weight. This solution reduced the number of evaluation of about 2000 initially at 12. Henceforth, an optimization process is possible.

The PMSM model permits to define variables of the optimization which are the electromagnetic parameters of the PMSM machine – *EMF* and reactances X_d and X_q. We choose to compare two cases linked to the saliency ratio – Normal-Saliency and Inverse-Saliency PMSM.

An optimization of each case has been carried out to compare optimal solution and to evaluate the saving of one versus the other. The minimizing of the current consumption was chosen as objective function, thus the vehicle's autonomy is maximized.

Results showed that the *EMF* and the difference between reactance must be maximized for VE application; moreover, we can estimate values of the electromagnetic parameters. And we demonstrate that the Inverse-Saliency PMSM is better to maximize VE autonomy.

REFERENCES

[1] C. C. Chan, "The State of the Art of Electric and Hybrid Vehicles", Proceding of the IEEE, Vol.90, No.2, pp 247-275 Februay 2002.

[2] M. Zeraoulia, M. E. H Benbouzid and D. Diallo, "Electric Motor Drive Selection Issues for HEV Propulsion Systems: A comparative Study", IEEE Transactions on Vehicular Technology, Vol.55, No.6, pp 1756-1764 November 2006.

[3] X. D. Xu, K. W. E. Cheng and N. C. Cheung, "Selection of Electric Motor Drives for Electric Vehicles", Power Engineering Conference 2008, AUPEC'08, Australasian Universities, 14-17 December 2008.

[4] P. H. Nguyen, E. Hoang, M. Gabsi, L Kobylansky and D. Condamin, "Permanent Magnet Synchronous Machines with Concentrated Flux and Fractional Slot Windings: Performances during Cycles for Hybrid Electric Vehicle Apllication", International Symposium on Industrial Electronics 2010 (ISIE), Bari, 4-7 july 2010.

[5] G. R. Slemon, "Achieving a constant power speed range for PM drives", IEEE Transactions on Industry Applications, Vol.31, No.2, pp 368-372, March/April 1995.

[6] J.SAINT-MICHEL, "Electric machines for hybrid vehicles applications", AEA 2006, Poitiers-Futuroscope, France, 5-6 April 2006.

[7] R. H. Staunton and all, "PM Motor Parametric Design Analyses for a Hybrid Electric Vehicle Traction Drive Application", OAK Ridge National Laboratory, Tenesse, USA, September 2004.
[8] R. F. Schiferl and T. A. Lipo, "Power Capability of Salient Pole Permanent Magnet Synchronous Motors in Variable Speed Drive", IEEE Transactions on Industry Applications, Vol.26, No.1, pp 115-123, January/February 1990.
[9] N. Bianchi, S. Bolognani and B. J. Chalmers, "Salient-rotor PM Synchronous Motors for an extended flux weakening operation range", IEEE Transactions on industry applications, Vol.36, No. 4, pp 1118-1125, July/August 2000.
[10] M. Hippner, R. G. Harley, "Looking for an optimal rotor for high speed permanent magnet synchronous machine", Conference Record of the IEEE Industry Applications Society Annual Meeting, vol.1, pp265-270, 1992.

***Authors**: Benjamin Dagusé is with École Supérieure d'Électricité, 3 rue Joliot-Curie, F-91192 Gif-sur-Yvette, France, E-mail: benjamin.daguse@supelec.fr; Philippe Dessante is with École Supérieure d'Électricité, 3 rue Joliot-Curie, F-91192 Gif-sur-Yvette, France, E-mail: philippe.dessante@supelec.fr; Pierre Vidal is with École Supérieure d'Électricité, 3 rue Joliot-Curie, F-91192 Gif-sur-Yvette, France, E-mail: pierre.vidal@supelec.fr; Jean-Claude Vannier is with École Supérieure d'Électricité, 3 rue Joliot-Curie, F-91192 Gif-sur-Yvette, France, E-mail : jean-claude.vannier@supelec.fr; Jacques Saint-Michel is with Moteurs Leroy Somer, Scientific Direction, F-16000 Angoulême, France ; Jean-Luc Thomas is with École Supérieure d'Électricité, 3 rue Joliot-Curie, F-91192 Gif-sur-Yvette, France.*